TGF-β1 promotes microglial amyloid-β clearance and reduces plaque burden in transgenic mice

Tony Wyss-Coray[1,2], Carol Lin[1], Fengrong Yan[1], Gui-qiu Yu[1], Michelle Rohde[1],
Lisa McConlogue[4], Eliezer Masliah[5] & Lennart Mucke[1,2,3]

[1]Gladstone Institute of Neurological Disease, [2]Department of Neurology and [3]Neuroscience Program,
University of California, San Francisco, California, USA
[4]Elan Pharmaceuticals, South San Francisco, California, USA
[5]Departments of Neurosciences and Pathology, University of California, San Diego, La Jolla, California, USA
Correspondence should be addressed to T.W.-C.; email: twysscoray@gladstone.ucsf.edu

Abnormal accumulation of the amyloid-β peptide (Aβ) in the brain appears crucial to pathogenesis in all forms of Alzheimer disease (AD), but the underlying mechanisms in the sporadic forms of AD remain unknown. Transforming growth factor β1 (TGF-β1), a key regulator of the brain's responses to injury and inflammation, has been implicated in Aβ deposition *in vivo*. Here we demonstrate that a modest increase in astroglial TGF-β1 production in aged transgenic mice expressing the human β-amyloid precursor protein (hAPP) results in a three-fold reduction in the number of parenchymal amyloid plaques, a 50% reduction in the overall Aβ load in the hippocampus and neocortex, and a decrease in the number of dystrophic neurites. In mice expressing hAPP and TGF-β1, Aβ accumulated substantially in cerebral blood vessels, but not in parenchymal plaques. In human cases of AD, Aβ immunoreactivity associated with parenchymal plaques was inversely correlated with Aβ in blood vessels and cortical TGF-β1 mRNA levels. The reduction of parenchymal plaques in hAPP/TGF-β1 mice was associated with a strong activation of microglia and an increase in inflammatory mediators. Recombinant TGF-β1 stimulated Aβ clearance in microglial cell cultures. These results demonstrate that TGF-β1 is an important modifier of amyloid deposition *in vivo* and indicate that TGF-β1 might promote microglial processes that inhibit the accumulation of Aβ in the brain parenchyma.

AD is a progressive dementing illness characterized by excessive accumulation of extracellular Aβ in the forms of amyloid plaques in the brain parenchyma and Aβ deposits in the cerebrovasculature[1,2]. The proteolytic cleavage of APP produces two major forms of Aβ: the 40–amino-acid variant $A\beta_{1-40}$, which is the major form secreted by cells; and the 42–amino-acid variant $A\beta_{1-42}$, which aggregates more quickly and is more neurotoxic[1]. $A\beta_{1-42}$ seems to be the main species found in early, diffuse deposits, whereas $A\beta_{1-40}$ accumulates later. However, it is unclear what factors initiate the deposition of these Aβ species in plaques or blood vessels.

Accumulation of Aβ might result from increases in its production, aggregation or deposition, or from its decreased clearance. Mutations in the APP or presenilin genes that lead to increased production of Aβ cause familial autosomal dominant forms of AD (ref. 1). In addition, increased production of hAPP/Aβ in transgenic mice results in age-related development of AD-type pathology, including amyloid plaques (refs. 3–5). Aβ production in brain also increases after head trauma, which may explain why traumatic brain injury is a risk factor for AD (refs. 6,7). However, familial mutations or traumatic brain injury are present in only a small fraction of AD cases, and in most patients Aβ production does not appear to be markedly elevated. It is possible that abnormal deposition of Aβ in the AD brain is due to processes that increase the aggregation of Aβ after it has been released into the extracellular milieu and/or processes that decrease the clearance of Aβ deposits.

One putative mechanism of Aβ clearance involves transport by apolipoprotein E or J into the blood or lymph nodes[8]. Ablation of mouse apolipoprotein E expression[9] or overexpression of human apolipoprotein E (ref. 10) decreased Aβ deposition and altered the distribution of Aβ in the brain, but the underlying mechanisms of these effects remain unknown. Activated microglia might contribute to the degradation and clearance of Aβ (refs. 11–13). After immunization of APP transgenic mice with synthetic $A\beta_{1-42}$ (refs. 14,15), microglia are stimulated to phagocytose and clear Aβ deposits. However, there is evidence that activated microglia might have detrimental roles in AD (refs. 16,17). To harness microglial activities for potential therapies, it will be advantageous to identify regulators that can tilt the balance of their activities towards neuroprotection in specific pathophysiological situations.

The multifunctional cytokine TGF-β1 is a potent regulator of injury and inflammatory responses in the CNS (central nervous system)[18] and has been implicated in cerebral amyloid deposition[19,20] and AD pathogenesis[18,21,22]. Cerebral TGF-β1 mRNA levels correlate positively with the extent of amyloid deposition in cerebral blood vessels in AD cases[19], and astroglial overproduction of TGF-β1 in hAPP mice promotes the deposition of human Aβ in cerebral blood vessels[19]. At least some of these effects might be mediated through the prominent induction of extracellular matrix proteins by TGF-β1 *in vivo*[23–25]. Using hAPP/TGF-β1 bigenic mice, we demonstrate here that, in con-
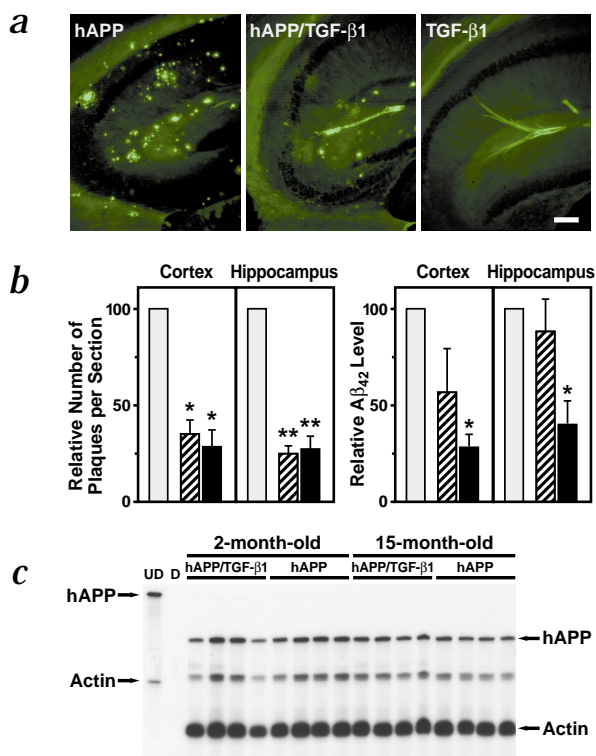
Fig. 1 TGF-β1 reduces amyloid plaque burden and inhibits Aβ accumulation in brain parenchyma. ***a***, Thioflavin S staining of the hippocampus revealed many fewer parenchymal plaques in hAPP/TGF-β1^{Low} than in hAPP mice. Vascular amyloid was not apparent in hAPP mice but prominent in hAPP/TGF-β1^{Low} and TGF-β1^{Low} mice. Scale bar: 200 μm. ***b***, Relative numbers of plaques and Aβ$_{1-42}$ levels in neocortex and hippocampus of hAPP (▨), hAPP/TGF-β1^{Low} (▨), and hAPP/TGF-β1^{Medium} (■) mice (6–8 mice/group). *, $P < 0.05$; **, $P < 0.005$ versus hAPP mice (Mann-Whitney U test). Measurements in hAPP/TGF-β1 mice (mean ± s.e.m.) were normalized to the mean value obtained in hAPP littermates (arbitrarily defined as 100%). ***c***, Representative autoradiograph shows similar levels of hAPP mRNA expression in the different genotypes and age groups. UD, undigested probes; D, digested probes in the absence of sample mRNA. The hAPP probe detects human but not mouse APP; it also recognizes an SV40 segment (middle band) of transgene-derived mRNAs.

TGF-β1 decreases plaque burden and overall Aβ load in brain

To determine how TGF-β1 affects human Aβ deposition *in vivo*, we crossed hAPP transgenic mice (platelet-derived growth factor (PDGF)-hAPP$^{K670N, M671L, V717F}$ line J9)[29,30], expressing hAPP and Aβ in neurons at high levels with transgenic mice expressing TGF-β1 in astrocytes[19,24,25,28]. At 8–10 months of age, hAPP singly transgenic mice develop compact Aβ deposits (amyloid plaques) in the brain parenchyma[29,30] that can be identified by staining with thioflavin S. At 12–15 months of age, hAPP mice had an average of 90 thioflavin-S–positive plaques per sagittal brain section, but very few vascular Aβ deposits (Fig. 1). In contrast, hAPP/TGF-β1 bigenic mice overexpressing TGF-β1 at low (line T64, TGF-β1^{Low}) or medium (line T115, TGF-β1^{Medium}) levels[24] had 65–75% fewer plaques (Fig. 1b). Consistent with our previous findings in 2–3-month-old hAPP/TGF-β1 mice[19], 12–15-month-old hAPP/TGF-β1 mice had predominantly cerebrovascular amyloid deposits (Fig. 1a).

The above findings raised the question of whether TGF-β1 merely induced a redistribution or change in local accumulation of the deposits (that is, from parenchyma to blood vessels), or if it actually inhibited the overall accumulation of Aβ. To address the latter possibility, we analyzed the overall amyloid load in the hippocampus, the area affected most severely by amyloid deposi-

trast to its amyloidogenic effects on the cerebral vasculature, TGF-β1 strongly reduces the overall cerebral Aβ load by inhibiting the formation of neuritic plaques in the brain parenchyma. Three lines of evidence indicate that this effect of TGF-β1 might be mediated by activated microglia: as a chemoattractant for macrophages/microglia, TGF-β1 increased microglial activation[26–28]; the reduced plaque burden in old hAPP/TGF-β1 mice was associated with widespread microglial activation; and TGF-β1 stimulated cultured microglial cells to clear synthetic Aβ.

Fig. 2 Change in distribution and overall decrease in hippocampal Aβ deposits in hAPP/TGF-β1 mice. ***a–i***, Sagittal brain sections of 12-month-old hAPP (*a*, *f* and *g*) and hAPP/TGF-β1^{low} mice (*b–e*, *h* and *i*) were stained for human Aβ deposition with antibodies against Aβ$_{1-5}$ (3D6 antibody; *a–e*), Aβ$_{40}$ (FCA3340 antibody; *f* and *h*), or Aβ$_{42}$ (FCA3542 antibody; *g* and *i*). Antibody binding was visualized with horseradish peroxidase (*a–c* and *f–i*) or FITC-tagged secondary antibodies (*d* and *e*). *a* and *b*, Aβ deposition in the hippocampal stratum oriens and in the outer molecular layer of the dentate gyrus (open arrowheads) is prominent in hAPP (*a*) but not hAPP/TGF-β1^{Low} brain (*b*). The latter shows dense staining in the hippocampal fissure and the meninges (filled arrowheads). *c*, Enlargement of the boxed area in (*b*) shows mostly diffuse Aβ deposits associated with vascular structures (several vessels are traced in blue). *d* and *e*, Details of Aβ deposits associated with medium-size blood vessels (*d*) and microvessels (*e*). *f–i*, The deposits labeled by the Aβ$_{40}$ antibody in hAPP and hAPP/TGF-β1 mice were more compact (*f* and *h*) than those labeled by the Aβ$_{42}$ antibody (*g* and *i*) (area shown is the molecular layer of the dentate gyrus). *h* and *i*, In hAPP/TGF-β1 mice, both antibodies labeled vascular elements (arrows point to vessels). Scale bars: 500 μm (*a* and *b*), 100 μm (*c*), 20 μm (*d* and *e*) and 50 μm (*f–i*).
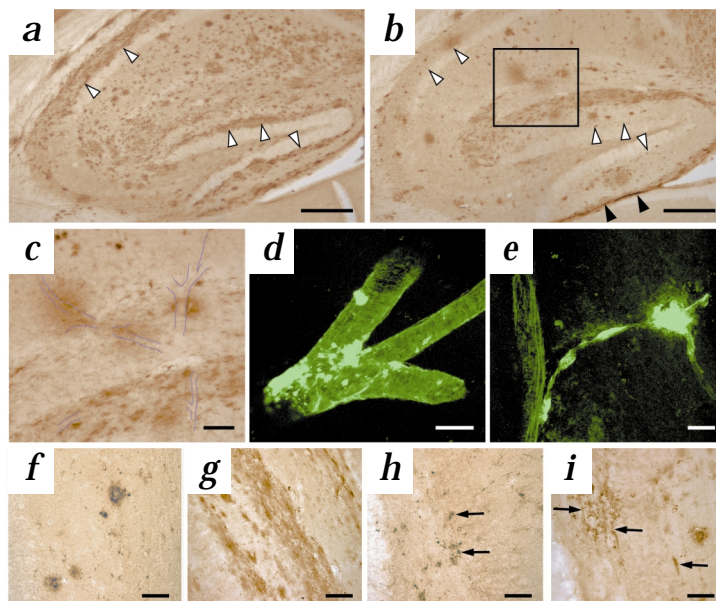
Fig. 3 Localization of Aβ deposits along blood vessels in hAPP/TGF-β1 mice. Sagittal brain sections from 12-month-old hAPP/TGF-β1^{Low} or hAPP mice were double-labeled and pseudo-colored for blood vessels (anti-Glut-1, red) and human Aβ (anti-3D6, green) and analyzed by confocal microscopy. Projections of 20 consecutive confocal images collected at 1.5-μm intervals. The merged images show the preferential localization of Aβ deposits along blood vessels in the hippocampus of the hAPP/TGF-β1^{Low} (bottom) but not the hAPP mouse (top). Note also the lower amount of parenchymal Aβ deposition in the hAPP/TGF-β1^{Low} brain. Scale bar: 100 μm.
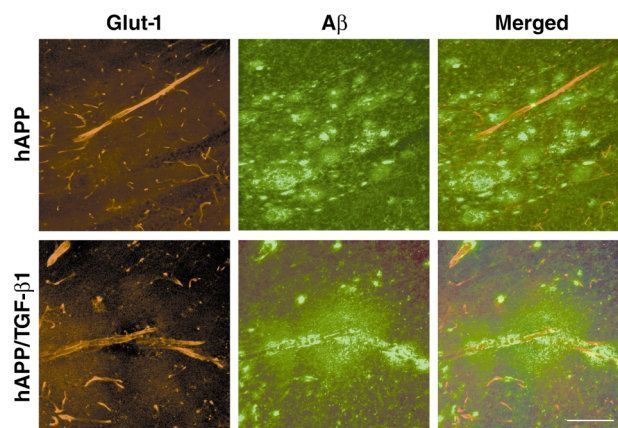
tion in hAPP mice[3,30]. Quantitative immunohistochemistry with antibodies specific for human Aβ revealed that the total area of the hippocampus occupied by Aβ deposits was much smaller in hAPP/TGF-β1^{Low} mice ($n = 5$) than in hAPP mice ($n = 4$). We observed this effect with the antibody FCA3340 (ref. 31) specific for the carboxy terminus of Aβ$_{40}$ (60% reduction; $P = 0.03$) and with antibody 3D6 (ref. 32) specific for the amino terminus of Aβ (61% reduction; $P = 0.02$).

We confirmed these results biochemically by measuring the levels of Aβ$_{1-x}$ (approximates total Aβ) or Aβ$_{1-42}$ in the hippocampus or neocortex by ELISA. Inhibition of plaque formation in both brain regions in 12–15-month-old hAPP/TGF-β1^{Medium} mice was associated with a 60–70% decrease in Aβ$_{1-42}$ and Aβ$_{1-x}$ levels (Fig. 1b and Table 1). Even at lower levels of TGF-β1 expression, the number of thioflavin-S–positive plaques in hAPP/TGF-β1^{Low} mice was reduced by 70% in hippocampus and neocortex (Fig. 1b). At 12–15 months, the relative proportion of cortical Aβ made up by Aβ$_{1-42}$ was significantly lower in hAPP/TGF-β1^{Medium} mice than in hAPP mice (Table 1).

The inhibition of Aβ accumulation and the change in distribution of Aβ deposits in hAPP/TGF-β1 mice might be due to effects of TGF-β1 on production, aggregation or clearance of Aβ. TGF-β1 did not alter cerebral hAPP mRNA expression in young or old mice (Fig. 1c) and did not change steady-state levels of Aβ in young mice at an age when no plaques were detected (Table 1). Likewise, expression of hAPP did not alter TGF-β1 transgene levels or endogenous TGF-β1 mRNA levels in bigenic mice (data not shown). These results indicate that TGF-β1 does not change the expression of PDGF-hAPP transgene products and does not significantly alter the production of soluble Aβ.

TGF-β1 decreases plaque-associated neurodegeneration

In AD and in hAPP mice, dense amyloid plaques often are associated with dystrophic neurites that can be identified by the presence of hyperphosphorylated tau and their characteristic morphological features[2,33]. hAPP/TGF-β1^{Low} mice had significantly fewer dystrophic neurites than hAPP mice (67% reduction; $P = 0.02$; $n = 7$ mice per group) as assessed by immunostaining with the AT8 antibody specific for hyperphosphorylated tau. Although this might simply reflect a decrease in the number of mature plaques (which contain dystrophic neu-

rites), it is important to note that TGF-β1 is a potent neuroprotective factor[21]. Hence, if neuronal damage is a prerequisite for Aβ seeding or accumulation and precedes plaque formation[29,30], reducing this damage through increased production of neuroprotective factors might prevent plaque formation.

Inverse correlation between Aβ deposits in plaques and vessels

Compared with hAPP mice, hAPP/TGF-β1 mice showed not only less Aβ immunoreactivity but also a distinctly different pattern of Aβ deposition (Fig. 2a and b). In hAPP mice, Aβ deposits were prominent in the stratum oriens of the hippocampus, the molecular layer of the dentate gyrus and the subiculum (Fig. 2a). In hAPP/TGF-β1 mice, these areas showed only sparse deposition of Aβ, and remaining Aβ deposits in the parenchyma were located primarily in the hippocampal fissure and the meninges (Fig. 2b). Thus, Aβ deposits in hAPP/TGF-β1 mice coincided with regions containing a high density of cerebral blood vessels in rodents[34]. Diffuse plaques in these mice formed mostly in the vicinity of medium-size blood vessels and capillaries (Figs. 2 and 3), whereas Aβ deposits in hAPP mice did not show this clear association with the vasculature (Fig. 3). In hAPP and hAPP/TGF-β1 mice, Aβ$_{40}$ immunoreactivity was associated primarily with dense deposits whereas Aβ$_{42}$ immunoreactivity was distributed more diffusely (Fig. 2f-i), consistent with findings in human brains[35,36]. In hAPP/TGF-β1 mice, Aβ$_{40}$ and Aβ$_{42}$ immunostaining frequently colocalized with vascular structures (Fig. 2h and i). A more detailed biochemical analysis of parenchymal and vascular Aβ deposits will be required to determine whether there might be a preferential deposition of Aβ$_{1-40}$ in cerebral blood vessels, as seen in other hAPP mouse models and certain patients with AD (refs. 35,36).

Quantification of amyloid deposits in plaques and blood vessels of hAPP and hAPP/TGF-β1 mice revealed nonoverlapping data clouds (Fig. 4a), further indicating that TGF-β1 could have

		Neocortex			Hippocampus		
Mice		Aβ$_{1-x}$ (ng/g)	Aβ$_{1-42}$ (ng/g)	%Aβ$_{1-42}$	Aβ$_{1-x}$ (ng/g)	Aβ$_{1-42}$ (ng/g)	%Aβ$_{1-42}$
2-month-old	hAPP	60.3 ± 4.4	18.1 ± 1.8	28 ± 1	169 ± 10.1	29.6 ± 2.6	17 ± 1
	hAPP/TGF-β1	61.2 ± 3.5	17.8 ± 1.6	28 ± 1	168 ± 10.3	30.6 ± 2.8	18 ± 1
12–15-month-old	hAPP	2037 ± 559	1610 ± 492	70 ± 5	4702 ± 1335	3827 ± 250	80 ± 1
	hAPP/TGF-β1	730 ± 141*	439 ± 117*	52 ± 6*	1943 ± 591	1519 ± 4929*	71 ± 5

Table 1 Aβ levels in brain regions of young and old mice

*, $P < 0.05$ versus age-matched hAPP mice (Mann-Whitney U test).

Fig. 4 Inverse correlation between Aβ deposits in blood vessels and plaques and association with TGF-β1 expression levels in brains from mice and AD cases. *a*, Sagittal brain sections from 12–15-mo-old hAPP (*n* = 9; open circles) and hAPP/TGF-β1^{Low} (*n* = 8; closed circles) mice were stained with thioflavin S, and hippocampal plaques and vessels were counted. Each circle represents the average numbers from 5–6 sections per mouse. hAPP/TGF-β1 mice had more amyloid in blood vessels (*P* < 0.0001) and less amyloid in plaques (*P* = 0.0002) than hAPP mice (Mann-Whitney U test). *b–e*, Brain tissue from the mid-frontal gyrus of AD cases with various degrees of cerebrovascular amyloid deposits was divided and either sectioned with a vibratome for immunohistochemical (anti-human Aβ; *b, d* and *e*) or histochemical (thioflavin S; *c*) analysis or homogenized and analyzed for TGF-β1 mRNA levels by RNase protection assay (*c* and *d*). *b*, Significant inverse correlation between Aβ deposits associated with plaques or blood vessels in AD (logarithmic regression analysis) as determined by the percent area occupied by Aβ-immunoreactive plaques or vessels. Each triangle represents average values from 3 sections per case and 2 randomly selected fields per section. Cases with very low overall Aβ deposition (total Aβ immunoreactive area occupied < 3%) were excluded from the analysis. *c*, Significant positive correlation between relative severity of CAA determined by thioflavin-S staining and TGF-β1 mRNA levels (Spearman rank test). *d*, Significant inverse correlation between Aβ deposits associated with plaques and TGF-β1 mRNA levels (logarithmic regression analysis). *e*, 2 AD cases with Aβ deposition preferentially in plaques (left) or along blood vessels (right). Scale bar: 200 µm.
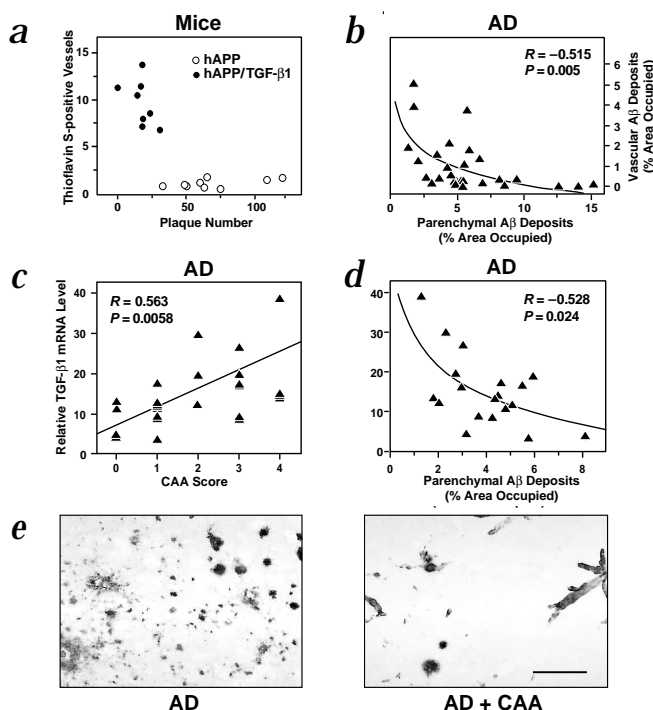
opposing effects on human Aβ deposition in blood vessels and brain parenchyma. To determine whether TGF-β1 has similar effects in AD brains, we analyzed the relationship between TGF-β1 levels and amyloid deposits in cerebral blood vessels versus parenchymal plaques. In 28 cases with AD (Blessed score > 10; see Methods) we found highly significant inverse correlations between Aβ immunoreactivity in plaques and cerebral blood vessels (Fig. 4*b*) and between Aβ immunoreactivity in plaques and

the severity of cerebral amyloid angiopathy (CAA) (*R* = –0.613, *P* = 0.0004 by Spearman rank correlation). Consistent with our previous observations[19], CAA severity correlated positively with TGF-β1 mRNA levels (Fig. 4*c*), as well as with Aβ immunoreactivity in the blood vessels (*R* = 0.774, *P* < 0.0001 by Spearman rank correlation). In contrast, the relative amount of Aβ in parenchymal plaques correlated inversely with TGF-β1 mRNA levels (Fig. 4*d*). Some AD cases had essentially no cerebrovascular amyloidosis or CAA with deposition of Aβ almost exclusively in plaques (Fig. 4*e*, left panel). In contrast, AD cases with severe CAA often had relatively little amyloid deposition in plaques (Fig. 4*e*, right panel), consistent with previous findings[37].

In summary, AD cases with severe CAA had higher TGF-β1 mRNA levels and a lower plaque burden, whereas AD cases with little vascular amyloid had lower TGF-β1 mRNA levels and more
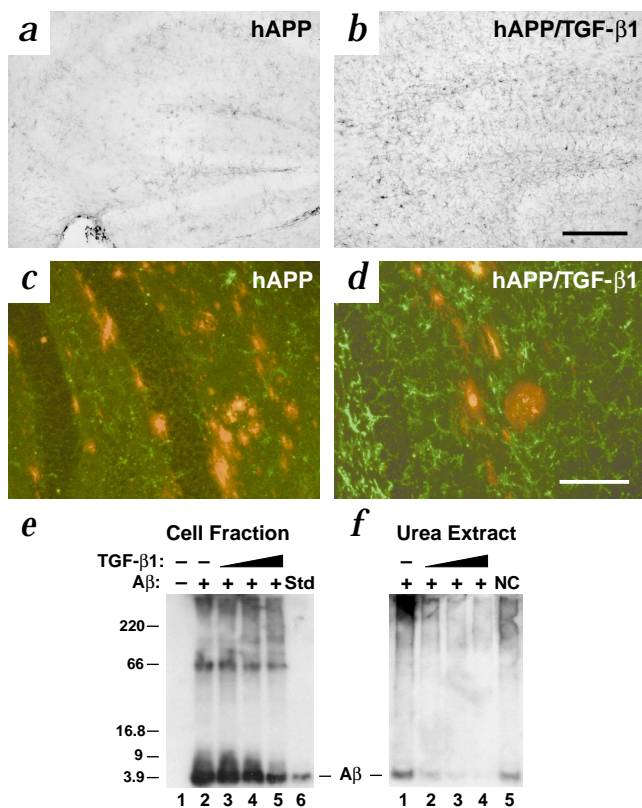

Fig. 5 TGF-β1 increases microglia activation in aged hAPP/TGF-β1 mice and promotes Aβ clearance in cell culture. *a* and *b*, Sagittal brain sections from 15-month-old hAPP and hAPP/TGF-β1^{Low} mice stained for microglia (anti-F4/80) using horseradish peroxidase. Scale bar: 500 µm. *c* and *d*, Brain sections from the same mice were double-labeled and pseudo-colored for microglia (anti-F4/80, green) and human Aβ (anti-3D6, red). Merged images show an abundance of Aβ deposits paired with weak microglia staining in the hAPP mouse (*c*), as opposed to sparse Aβ deposition and intense microglial labeling in the hAPP/TGF-β1^{Low} mouse (*d*). Scale bar: 50 µm. *e*, BV-2 microglial cells were exposed to synthetic Aβ$_{1-42}$ (lanes 2–5) or not (lane 1) and stimulated with different concentrations of recombinant TGF-β1 (0.1, 1 and 10 ng/ml in lanes 3, 4 and 5, respectively). Western-blot analysis of cell fractions with an antibody against human Aβ$_{13-28}$ (266) showed a TGF-β1–dependent decrease in cell-associated Aβ. This decrease was not associated with an increased formation of Aβ aggregates (Mr > 16.8 kD). In lane 6, synthetic Aβ$_{1-42}$ was loaded as a standard (Std). *f*, Total Aβ (assessed using 266 antibody) in whole-culture extract (using 8 M urea) from BV-2 microglial cultures stimulated as above. Western-blot analysis of this extract showed a TGF-β1–dependent decrease in Aβ (lanes 2–4). TGF-β1 added at the maximum concentration in the absence of microglia (lane 5; NC, no cells) did not result in such a decrease in Aβ (compare lanes 4 and 5).

parenchymal plaques, suggesting that TGF-β1 exerts effects in the AD brain similar to those in hAPP/TGF-β1 mice.

TGF-β1 induces activation of microglia and clearance of Aβ

As microglia have been implicated in the clearance of Aβ aggregates[11–13], we assessed their activation state in our models. Compared with age-matched hAPP, TGF-β1 and nontransgenic mice, 12–15-month-old hAPP/TGF-β1 mice displayed a prominent and widespread activation of microglia, as demonstrated by increased immunolabeling with the F4/80 marker and typical morphological changes (Fig. 5a–d). No change in microglial activation was seen in young bigenic mice (data not shown). At 15 months, mRNA levels of the microglial product, macrophage inflammatory protein 1α (MIP-1α), were increased two-fold in hAPP mice and three-fold in hAPP/TGF-β1 mice compared with nontransgenic littermate controls (nontransgenic = 147 ± 35; TGF-β1 = 191 ± 52; hAPP = 357 ± 62; hAPP/TGF-β1 = 517 ± 127; values are mean ± s.e.m. of mRNA measurements from cortices of 3–5 mice per genotype; $P < 0.05$ by Kruskal-Wallis in hAPP/TGF-β1 versus nontransgenic or TGF-β1). These data provide further evidence for an increased activation of microglia in the bigenic mice.

To test whether TGF-β1 stimulates microglia to inhibit Aβ accumulation, we exposed cultured BV-2 microglial cells to synthetic Aβ$_{1-42}$ in the presence or absence of recombinant TGF-β1. After 18 hours, the Aβ content of cell fractions (Fig. 5e) and cell-culture supernatants (data not shown) was determined by western-blot analysis. TGF-β1 induced a dose-dependent clearance of Aβ peptide from the cultures. Similar results were also obtained when cultures were extracted directly with 8 M urea and then analyzed by western blotting (Fig. 5f). The effect of TGF-β1 on Aβ in these cultures was mediated by microglia, as TGF-β1 did not reduce Aβ levels significantly in the absence of microglia (Fig. 5f).

Discussion

Abnormal accumulation of Aβ is considered a key pathogenic mechanism in AD, but little is known about its molecular basis in sporadic AD, the most common form of this illness. A better understanding of the processes that regulate Aβ accumulation in the brain could facilitate the development of treatments to prevent or inhibit the accumulation of amyloid in AD. We show here that the cytokine TGF-β1 strongly decreases amyloid-plaque burden and neuritic pathology in hAPP/TGF-β1 bigenic mice. In addition, TGF-β1 altered the pattern of Aβ deposition, promoting deposition along cerebral blood vessels. The net result of astroglial TGF-β1 overexpression was a significant reduction in the overall Aβ content of the brain. This reduction seems to involve, at least in part, activation of microglial cells.

Although TGF-β1 plays an essential role in the normal repair processes after tissue injury[23], excessive production of TGF-β1 promotes tissue fibrosis in a number of diseases including liver cirrhosis, pulmonary fibrosis, fibrotic kidney disease[38] and hydrocephalus[24,39]. These findings underscore the multi-functionality of TGF-β1 and the dependence of its effects on the particular cellular environment and pathophysiological scenario in which it is expressed. TGF-β1 is increased several-fold after acute brain injury[21,22]. The acute overproduction of TGF-β1 in the brain, mainly by astrocytes and microglia, is thought to organize repair processes and to protect neurons from degeneration[18,21]. In TGF-β1 mice, however, chronic overproduction of TGF-β1 in the brain results in cerebrovascular amyloidosis and degenera-

tion[19,25]. Cerebral TGF-β1 levels are higher in AD cases than in nondemented controls, and TGF-β1 immunoreactivity is increased in plaques and perivascular astrocytes[21,22]. Cortical TGF-β1 mRNA levels in AD cases correlate positively with the degree of CAA (ref. 19; Fig. 4), but inversely with deposition of Aβ in plaques (Fig. 4), suggesting that increased production of TGF-β1 promotes deposition of Aβ in cerebral blood vessels but reduces plaque formation in the brain parenchyma. These findings indicate that TGF-β1 is a key regulator of Aβ deposition in the brain.

Because of the multi-functionality of TGF-β1 and the complex interactions between different types of CNS cells *in vivo*, a considerable amount of additional investigation will be necessary to characterize all cellular and molecular processes involved in the redistribution and overall clearance of amyloid induced by TGF-β1. Several lines of evidence indicate that differential effects of TGF-β1 on astrocytes along blood vessels and on microglial in the brain parenchyma may play important roles.

Overproduction of TGF-β1 activates astrocytes—most prominently around cerebral blood vessels[24]. Activation of perivascular astrocytes is followed by the accumulation of basement membrane proteins and the deposition of amyloid in cerebral blood vessels of TGF-β1 mice[24,25], supporting the concept that extracellular-matrix proteins provide the seed for amyloid formation[40]. Thus, high levels of extracellular matrix proteins in blood vessels could increase the affinity of Aβ to the vasculature and promote cerebrovascular amyloidosis. Some of the vascular Aβ might be cleared along periarterial interstitial fluid-drainage channels into lymph nodes[37], lowering the overall load of Aβ in the brain. Support for such a scenario also comes from APP transgenic mice that accumulate neuron-derived Aβ in prominent cerebrovascular amyloid deposits[41]. Astrocytes are also highly activated around cerebrovascular amyloid deposits in AD and CAA, whereas activated microglia are typically associated with parenchymal plaques but not with cerebrovascular amyloid deposits[42].

In contrast to the amyloidogenic effects of TGF-β1 on perivascular astrocytes and other vascular cells, effects of TGF-β1 on microglia likely counteract amyloid deposition. In aged hAPP/TGF-β1 mice, TGF-β1 overproduction resulted in a prominent microglial activation associated with a marked decrease in plaque load and overall amyloid burden in the brain (Fig. 5). TGF-β1 activates and attracts macrophages/microglia *in vivo*[26,27] and increases the recruitment of these cells to the CNS after immune challenge[28]. Microglia are thought to assist in the removal of cerebral Aβ by releasing Aβ-degrading enzymes[12] or by internalizing Aβ aggregates through cell-surface receptors[13], and they have been implicated in the clearance of Aβ deposits in hAPP transgenic mice immunized with synthetic Aβ (refs. 14,15). In contrast, other studies suggested that microglia contribute to Aβ deposition and plaque formation[17]. Our *in vitro* data indicate that TGF-β1 could stimulate the removal of Aβ by activating microglia-dependent clearance mechanisms. In combination with the TGF-β1–induced reduction in amyloid plaques, our results also raise the intriguing possibility that TGF-β1 might be involved in the removal of amyloid deposits following vaccination with Aβ.

Microglia are activated and a wide array of inflammatory proteins are expressed at elevated levels in the AD brain[22,43]. We show that TGF-β1-induced microglial activation is associated with a reduction in plaques and neuritic dystrophy, raising the possibility that certain inflammatory processes serve to inhibit AD-type pathology. Therefore, the pharmacological manipula-

tion of specific neurotoxic pathways will likely be a better therapeutic strategy in AD and related conditions than a more general suppression of inflammatory responses in the brain.

Methods

Transgenic mice. The generation of mice expressing TGF-β1 in astrocytes from the glial fibrillary acidic protein (GFAP) promoter has been described[24]. Two independent lines of TGF-β1 mice were used expressing TGF-β1 at low (TGF-β1[Low,] line T64) or medium (TGF-β1[Medium,] line T115) levels. Mice expressing hAPP from the PDGF B-chain promoter have also been described[3,19,29,30]. The PDGF-hAPP line J9 (hAPP mice)[29,30] selected for this study expresses an alternatively spliced minigene that encodes hAPP695, hAPP751 and hAPP770 bearing the amyloidogenic K670M/N671L and V717F mutations, which have been linked to familial AD (ref. 1). Heterozygous TGF-β1 mice on the BALB/c × SJL (cSJL) background were crossed with heterozygous hAPP mice on a C57BL/6 x DBA/2 (B6D2) background, and the resulting offspring (TGF-β1, hAPP, hAPP/TGF-β1, non-transgenic) were analyzed. Genomic DNA was extracted from tail biopsies and analyzed for TGF-β1 or hAPP transgenes with sequence-specific primers and PCR amplification as described[19].

AD cases. A total of 35 neuropathologically confirmed AD cases (Blessed score > 10; age 67–100 y; mean age 80 ± 1.4; postmortem intervals 2–18 h) with various degrees of CAA (0–4; 0 indicates no CAA, 4 indicates severe CAA as determined by inspection of thioflavin-S–labeled brain sections from the frontal neocortex[44]) from the Alzheimer's Disease Research Center of the University of California at San Diego were used in this study. Tissue samples obtained at autopsy from the midfrontal gyrus were fixed in freshly prepared 4% paraformaldehyde (pH 7.4) at 4 °C for 48 h and sectioned with a vibratome. Aβ deposits were stained and quantified as described below for mice. For each case, a tissue block from the same brain region was immediately snap-frozen and stored for RNA extraction.

Histology and immunohistochemistry. Mice were anesthetized with chloral hydrate and killed by transcardiac saline perfusion. Brains were removed rapidly and drop-fixed in phosphate-buffered 4% paraformaldehyde at 4 °C for 48 h for neuropathological analysis. Post-fixed brains were cut sagitally into 40-μm sections with a vibratome. Thioflavin-S staining was performed as described[19]. For each mouse, thioflavin-S–positive plaques or blood vessels were counted in 5 to 6 sections per hemibrain at a magnification of ×40. Individual images were also captured electronically and transferred to a Bioquant image analysis system (R&M Biometrics, Nashville, Tennessee) or to a Quantimet 570C imaging system (Leica, Deerfield, Illinois), and the number and area of plaques were measured as described[3,30]. Some images were analyzed by laser-scanning confocal microscopy with an Olympus BX60 microscope and a Radiance 2000 confocal setup (BioRad, Hercules, California). Images were pseudocolored with Photoshop software (Adobe, San Jose, California). For immunohistochemistry, brain sections from mice or AD cases were stained by standard immunoperoxidase techniques with ABC kits (Vector Labs, Burlingame, California) and 3,3′-diaminobenzidine plus hydrogen peroxide or by immunofluorescence-labeling procedures with FITC- and Cy5-tagged secondary antibodies[19] (Vector Labs). Sections were viewed by light microscopy, and images were captured with a Spot-2 camera (Diagnostic Instruments, Sterling Heights, Michigan), or by laser-scanning confocal microscopy. For some experiments, images were captured electronically and transferred to a Bioquant image analysis system to determine relative areas occupied by immunoreactive material. The following primary antibodies were used: 3D6 [3 μg/ml] against human Aβ$_{1-5}$ (ref. 32; Elan Pharmaceuticals, South San Francisco, California); FCA3340 [1:1000] against human Aβ$_{40}$ (ref. 31); FCA3542 [1:1000] against human Aβ$_{42}$ (ref. 31); F4/80 [1:60] against microglia F4/80 antigen (Serotec, Raleigh, North Carolina); Glut-1 [1:1000], anti–glucose-transporter-1 (Chemicon, Temecula, California); and AT8 [1:500] against phosphorylated tau (Biosource International, Camarillo, California). Antibodies FCA3340 and FCA3542 were provided by F. Checler. For double-immunostaining experiments involving F4/80 and 3D6, F4/80 fluorescent immunostaining was enhanced with a tyramide signal amplification kit (NEN, Boston, Massachusetts).

RNA extraction and analysis. Total RNA from snap-frozen AD-brain specimens or from mouse hemibrains or dissected brain regions was isolated with TRI reagent (Molecular Research Center, Cincinnati, Ohio). The quality of human RNA was assessed by the relative levels of 18S and 28S rRNA on agarose/formaldehyde gels and 7/35 cases were excluded due to poor RNA quality. Total RNA was analyzed by solution hybridization RNase protection assay (RPA) as described[19]. mRNA levels were quantified from phosphorimager readings of probe-specific signals corrected for RNA content/loading errors by normalization to β-actin signals. The following [^{32}P]-labeled antisense riboprobes were used to identify specific mRNAs (protected nucleotides (nt), GenBank accession number): murine β-actin (nt 480–559, #M18194), porcine TGF-β1 (nt 999–1412, #M23703), murine TGF-β1 (nt 500–752, #M13177); and human APP (nt 2468–2657, #X06989 of human APP fused with a NotI linker to nt 2532–2656, #M24914 of SV40). The porcine TGF-β1 riboprobe protects also a 280- and a 125-nt fragment of human TGF-β1 mRNA (nt 935–1215 and 1226–1351 of human TGF-β1, #X02812), but does not protect human TGF-β2 or human TGF-β3 transcripts.

Aβ ELISAs. Homogenization of snap-frozen hippocampi and cortices in 5 M guanidine buffer, and ELISA measurements of human Aβ$_{1-x}$ (approximates total Aβ) and Aβ$_{1-42}$ were performed as described[32]. For the detection of Aβ$_{1-x}$, a sandwich ELISA consisting of capture antibody 266 (anti-human Aβ$_{13-28}$) and biotinylated reporter antibody 3D6 (anti-human Aβ$_{1-5}$) were used. Hence, this assay measures levels of Aβ species ranging from amino-acid positions 1–28 or longer. Aβ$_{1-42}$ levels were measured with capture antibody 21F12 (anti-human Aβ$_{33-42}$) and biotinylated detection antibody 3D6. All antibodies were from Elan Pharmaceuticals.

Microglial cell cultures. Mouse BV-2 microglia cells (gift from E. Blasi) in serum-free neurobasal medium supplemented with N2 (GIBCO, Grand Island, New York) and 2 mM L-glutamine were exposed to synthetic Aβ$_{1-42}$ peptide (Bachem, Torrance, California) at 500 nM and various concentrations of recombinant TGF-β1 (Promega, Madison, Wisconsin). After 18 h, cell culture supernatants were collected and the adherent cells were solubilized in triple-lysis detergent buffer[25]. Supernatants and solubilized cell fractions were diluted in lithium dodecyl-sulfate sample buffer (Novex, San Diego, California) and separated on the same day under non-reducing conditions on 4–12% Bis-Tris gels with 2-(N-morpholino) ethane sulfonic acid (MES)/SDS running buffer (pH 7.2; Novex). To assess different stages of Aβ aggregation, the samples were not cleared of insoluble material by centrifugation, but loaded directly onto gels. Insoluble, aggregated Aβ does not enter the gel and can be detected at the top (Fig. 5). In some experiments, 8 M urea was added directly to the cell cultures to solubilize proteins. After transfer to 0.2-μm nitrocellulose membranes (BA-S 83; Schleicher und Schüll, Keene, New Hampshire), blots were boiled for 10 min, blocked with 5% non-fat dry milk/PBS buffer, and stained with antibody 266 or 3D6 (2 μg/ml, Elan Pharmaceuticals). Antibody binding was revealed with peroxidase-conjugated anti-mouse antibodies and an ECL chemiluminescence kit (Amersham).

Statistical analyses. For all histopathological analyses, brain tissue samples were coded to ensure objective assessment, and codes were not broken until the analysis was complete. All statistical analyses were performed with Statview software (SAS Institute, Cary, North Carolina).

1. Selkoe, D.J. Translating cell biology into therapeutic advances in Alzheimer's disease. *Nature* **399**, A23–A31 (1999).
2. Terry, R.D., Katzman, R., Bick, K.L. & Sisodia, S.S. *Alzheimer Disease.* 2nd edn. (Lippincott Williams & Wilkins, Philadelphia, 1999).
3. Games, D. *et al.* Alzheimer-type neuropathology in transgenic mice overexpressing

V717F β-amyloid precursor protein. *Nature* **373**, 523–527 (1995).

4. Hsiao, K. *et al.* Correlative memory deficits, Aβ elevation, and amyloid plaques in transgenic mice. *Science* **274**, 99–102 (1996).

5. Sturchler-Pierrat, C. *et al.* Two amyloid precursor protein transgenic mouse models with Alzheimer disease-like pathology. *Proc. Natl. Acad. Sci. USA* **94**, 13287–13292 (1997).

6. Nicoll, J.A.R., Roberts, G.W. & Graham, D.I. Apolipoprotein E ε4 allele is associated with deposition of amyloid β-protein following head injury. *Nature Med.* **1**, 135–137 (1995).

7. Guo, Z. *et al.* Head injury and the risk of AD in the MIRAGE study. *Neurology* **54**, 1316–1323 (2000).

8. Zlokovic, B.V. Cerebrovascular transport of Alzheimer's amyloid β and apolipoproteins J and E: Possible anti-amyloidogenic role of the blood-brain barrier. *Life Sci.* **59**, 1483–1497 (1996).

9. Bales, K.R. *et al.* Lack of apolipoprotein E dramatically reduces amyloid β-peptide deposition. *Nat. Genet.* **17**, 263–264 (1997).

10. Holtzman, D.M. *et al.* Expression of human apolipoprotein E reduces amyloid-β deposition in a mouse model of Alzheimer's disease. *J. Clin. Invest.* **103**, R15–R21 (1999).

11. Frautschy, S.A., Cole, G.M. & Baird, A. Phagocytosis and deposition of vascular β-amyloid in rat brains injected with Alzheimer β-amyloid. *Am. J. Pathol.* **140**, 1389–1399 (1992).

12. Qiu, W.Q. *et al.* Insulin-degrading enzyme regulates extracellular levels of amyloid β-protein by degradation. *J. Biol. Chem.* **273**, 32730–32738 (1998).

13. Yan, S.D., Roher, A., Schmidt, A.M. & Stern, D.M. Cellular cofactors for amyloid β-peptide-induced cell stress. Moving from cell culture to *in vivo*. *Am. J. Pathol.* **155**, 1403–1411 (1999).

14. Schenk, D. *et al.* Immunization with amyloid-β attenuates Alzheimer-disease-like pathology in the PDAPP mouse. *Nature* **400**, 173–177 (1999).

15. Bard, F. *et al.* Peripherally administered antibodies against amyloid β-peptide enter the central nervous system and reduce pathology in a mouse model of Alzheimer disease. *Nature Med.* **6**, 916–919 (2000).

16. Giulian, D. Microglia and the immune pathology of Alzheimer disease. *Am. J. Hum. Genet.* **65**, 13–18 (1999).

17. Frackowiak, J. *et al.* Ultrastructure of the microglia that phagocytose amyloid and the microglia that produce β-amyloid fibrils. *Acta Neuropathol.* **84**, 225–233 (1992).

18. Finch, C.E., Laping, N.J., Morgan, T.E., Nichols, N.R. & Pasinetti, G.M. TGF-β1 is an organizer of responses to neurodegeneration. *J. Cell. Biochem.* **53**, 314–322 (1993).

19. Wyss-Coray, T. *et al.* Amyloidogenic role of cytokine TGF-β1 in transgenic mice and Alzheimer's disease. *Nature* **389**, 603–606 (1997).

20. Frautschy, S.A., Yang, F., Calderón, L. & Cole, G. M. Rodent models of Alzheimer's disease: Rat Aβ infusion approaches to amyloid deposits. *Neurobiol. Aging* **17**, 311–321 (1996).

21. Flanders, K.C., Ren, R.F. & Lippa, C.F. Transforming growth factor-βs in neurodegenerative disease. *Prog. Neurobiol.* **54**, 71–85 (1998).

22. Akiyama, H. *et al.* Inflammation and Alzheimer's disease. Neuroinflammation Working Group. *Neurobiol. Aging* **21**, 383–421 (2000).

23. Roberts, A.B. & Sporn, M.B. Transforming growth factor-β, in *The Molecular and Cellular Biology of Wound Repair* 2nd edn. (ed. Clark, R.A.F.), 275–308 (Plenum, New York, 1996).

24. Wyss-Coray, T. *et al.* Increased central nervous system production of extracellular matrix components and development of hydrocephalus in transgenic mice overexpressing transforming growth factor-β1. *Am. J. Pathol.* **147**, 53–67 (1995).

25. Wyss-Coray, T., Lin, C., Sanan, D., Mucke, L. & Masliah, E. Chronic overproduction of TGF-β1 in astrocytes promotes Alzheimer's disease-like microvascular degeneration in transgenic mice. *Am. J. Pathol.* **156**, 139–150 (2000).

26. Wahl, S.M. Transforming growth factor beta (TGF-β) in inflammation: A cause and a cure. *J. Clin. Immunol.* **12**, 61–74 (1992).

27. Yao, J., Harvath, L., Gilbert, D. & Colton, C. Chemotaxis by a CNS macrophage, the microglia. *J. Neurosci. Res.* **27**, 36–42 (1990).

28. Wyss-Coray, T., Borrow, P., Brooker, M.J. & Mucke, L. Astroglial overproduction of TGF-β1 enhances inflammatory central nervous system disease in transgenic mice. *J. Neuroimmunol.* **77**, 45–50 (1997).

29. Hsia, A. *et al.* Plaque-independent disruption of neural circuits in Alzheimer's disease mouse models. *Proc. Natl. Acad. Sci. USA* **96**, 3228–3233 (1999).

30. Mucke, L. *et al.* High-level neuronal expression of Aβ$_{1-42}$ in wild-type human amyloid protein precursor transgenic mice: Synaptotoxicity without plaque formation. *J. Neurosci.* **20**, 4050–4058 (2000).

31. Barelli, H. *et al.* Characterization of new polyclonal antibodies specific for 40 and 42 amino acid-long amyloid β peptides: Their use to examine the cell biology of presenilins and the immunohistochemistry of sporadic Alzheimer's disease and cerebral amyloid angiopathy cases. *Mol. Med.* **3**, 695–707 (1997).

32. Johnson-Wood, K. *et al.* Amyloid precursor protein processing and Aβ$_{42}$ deposition in a transgenic mouse model of Alzheimer disease. *Proc. Natl. Acad. Sci. USA* **94**, 1550–1555 (1997).

33. Masliah, E. *et al.* Comparison of neurodegenerative pathology in transgenic mice overexpressing V717F β-amyloid precursor protein and Alzheimer's disease. *J. Neurosci.* **16**, 5795–5811 (1996).

34. Paxinos, G. *The Rat Nervous System.* 2nd edn. (Academic, San Diego, 1995).

35. Mann, D.M. *et al.* Predominant deposition of amyloid-β 42(43) in plaques in cases of Alzheimer's disease and hereditary cerebral hemorrhage associated with mutations in the amyloid precursor protein gene. *Am. J. Pathol.* **148**, 1257–1266 (1996).

36. Kuo, Y.-M. *et al.* Comparative analysis of Aβ chemical structure and amyloid plaque morphology of transgenic mice and alzheimer disease brains. *J. Biol. Chem.* (in press).

37. Weller, R.O. *et al.* Cerebral amyloid angiopathy. Amyloid β accumulates in putative interstitial fluid drainage pathways in Alzheimer's disease. *Am. J. Pathol.* **153**, 725–733 (1998).

38. Border, W.A. & Noble, N.A. TGF-β in kidney fibrosis: A target for gene therapy. *Kidney Int.* **51**, 1388–1396 (1997).

39. Galbreath, E., Kim, S.-J., Park, K., Brenner, M. & Messing, A. Overexpression of TGF-β1 in the central nervous system of transgenic mice results in hydrocephalus. *J. Neuropathol. Exp. Neurol.* **54**, 339–349 (1995).

40. Kisilevsky, R. Proteoglycans and other basement membrane proteins in amyloidoses. *Mol. Neurobiol.* **9**, 23–24 (1994).

41. Calhoun, M.E. *et al.* Neuronal overexpression of mutant amyloid precursor protein results in prominent deposition of cerebrovascular amyloid. *Proc. Natl. Acad. Sci. USA* **96**, 14088–14093 (1999).

42. Verbeek, M.M., Otte-Höller, I., Veerhuis, R., Ruiter, D.J. & De Waal, R.M.W. Distribution of Aβ-associated proteins in cerebrovascular amyloid of Alzheimer's disease. *Acta Neuropathol.* **96**, 628–636 (1998).

43. McGeer, P.L. & McGeer, E.G. Inflammation of the brain in Alzheimer's disease: Implications for therapy. *J. Leukocyte Biol.* **65**, 409–415 (1999).

44. Olichney, J.M. *et al.* The apolipoprotein E4 allele is associated with increased neuritic plaques and cerebral amyloid angiopathy in Alzheimer's disease and Lewy body variant. *Neurology* **47**, 190–196 (1996).